JOURNAL OF PROPULSION AND POWER
Vol. 25, No. 2, March–April 2009

Submerged Combustion and Two-Phase Exhaust Jet Instabilities

M. Linck,* A. K. Gupta,† and K. Yu‡
University of Maryland, College Park, Maryland 20742

DOI: 10.2514/1.35724

Compact liquid-fueled swirl-stabilized combustors using advanced fuel atomization techniques provide a potential solution to challenges associated with propulsion of submerged naval vehicles. The submerged pressurized operation of a combustor may alter the operational characteristics and performance of the combustor and also involves two-phase phenomena when the combustor exhaust gases interact with surrounding water. This work describes an investigation of swirl-stabilized flames created in a combustor featuring coannular swirling airflows under submerged conditions. A central atomization-air jet was used to atomize methanol fuel, providing great flexibility and control over fuel spray properties in a compact geometry. Direct photography was used to examine the global features of the flame. High-speed imaging was used to examine the two-phase shear-layer behavior of the exhaust jet from the combustor. Sound spectra associated with exhaust jets under different operational conditions were compared. Three nozzle geometries were examined, and the impact of nozzle geometry on the two-phase jet interaction was assessed. The two-phase interaction of the exhaust jet was found to depend heavily on the pressure drop over the exhaust nozzle. The dynamic behavior of the exhaust jet was buoyancy-driven at low-pressure drops and was affected by complex instability mechanisms at high-pressure drops. Nozzle features that have been shown to affect the behavior of single-phase jet shear-layer instability were found to have little effect in a two-phase situation. The instability mechanisms involved in the two-phase cases investigated here are shown to be significantly different from jets in single-phase cases. Evidence is presented that a pressure-wave interaction mechanism, similar to Richtmyer–Meshkov instability, may play an important role in the evolution of unstable structures at the two-phase interface when high combustor pressures are involved.

I. Introduction

THE technical challenges faced in underwater propulsion are unique to U.S. Navy vessels, and so efforts must be made to examine traditional and future underwater fleets for high performance with negligible exhaust plume signatures. Furthermore, there is a need for small autonomous underwater vehicles (AUVs). As has been demonstrated by the Central Intelligence Agency's Predator program, autonomous vehicles, capable of monitoring or intervening in critical situations, are quite effective. A similar type of vehicle designed for naval applications could help monitor coastlines, eavesdrop on radio and other communications traffic while concealed in shallow waters, or actively pursue and eliminate threats. Combustion systems can provide much higher volumetric power density than comparably sized electric motors and can potentially be lighter. A hot exhaust jet from a combustor can be used to propel a vehicle, either by being vented directly into the surrounding water or by powering a turbine that turns a propeller. Combustors designed to operate across a large turndown ratio could propel the vehicle at a range of speeds: quietly and slowly when necessary or at speeds comparable with those of surface vehicles.

Whether the combustion gases are used to turn a propeller or to propel the vehicle directly, exhaust jet instabilities, particularly those driven by instabilities in the combustor, are likely to alter the sound signature of the vehicle when the jet interacts with water, making the AUV more detectable and more difficult to control. Understanding the exhaust jet behavior will be crucial in designing a practical vehicle. This paper describes progress made in examining issues of direct relevance to this area of underwater propulsion.

Combustors designed for future AUV applications or for larger-scale underwater-propulsion applications must operate efficiently at a range of pressures. Previous work [1] has been done to describe the structure and dynamics of exhaust jets emerging from combustors that are operated at low pressure. The present work will discuss the behavior of exhaust jets emerging from a combustor at low pressure and at elevated pressure, creating unchoked and choked exhaust jets, respectively.

Control of flame stability and structure is always a concern. Swirl-stabilized flames have been found to have extremely useful characteristics, providing large turndown ratios, rapid fuel vaporization, and efficient mixing, thus allowing the design of compact and stable combustion systems [2–4]. The research results presented here describe the behavior of a swirl-stabilized methanol-fueled combustor, which features design elements found currently in compact high-energy density combustors such as those in gas turbine engines. Twin-fluid atomization was used to provide flexible fuel atomization. This feature allowed for a particularly compact design in which fuel could be effectively atomized under a wide range of conditions.

To examine combustion issues related to underwater propulsion, an optically accessible experimental test section was developed and constructed (see Fig. 1). The test section consisted of two chambers linked by a flow channel into which a nozzle was inserted. The upstream chamber functioned as a combustor, allowing a variety of diagnostics to be applied to flames in the combustor. Particle image velocimetry (PIV), phase Doppler particle analysis, planar laser-induced fluorescence, thermal imaging, and chemiluminescent measurements of selected species using an intensified charge-coupled-device camera could be used for detailed examination of flames in the combustor. The downstream chamber, which will be referred to as the mixing chamber, was designed to simulate submerged conditions. The mixing chamber, featuring a square cross section and transparent acrylic walls, allowed the two-phase interaction between the exhaust jet and water to be observed directly.

Received 16 November 2007; revision received 20 October 2008; accepted for publication 26 October 2008.

*Graduate Researcher, Mechanical Engineering, 2181 Glenn L. Martin Hall. Student Member AIAA.

†Distinguished University Professor, Mechanical Engineering, 2181 Glenn L. Martin Hall. Fellow AIAA.

‡Associate Professor, Aerospace Engineering, 3181 Glenn L. Martin Hall. Associate Fellow AIAA.

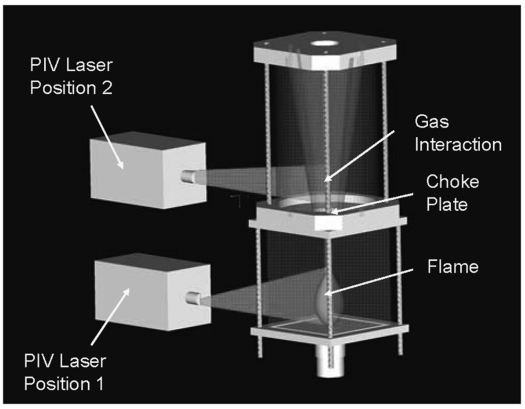

Fig. 1 Schematic of the test section for submerged combustion studies.

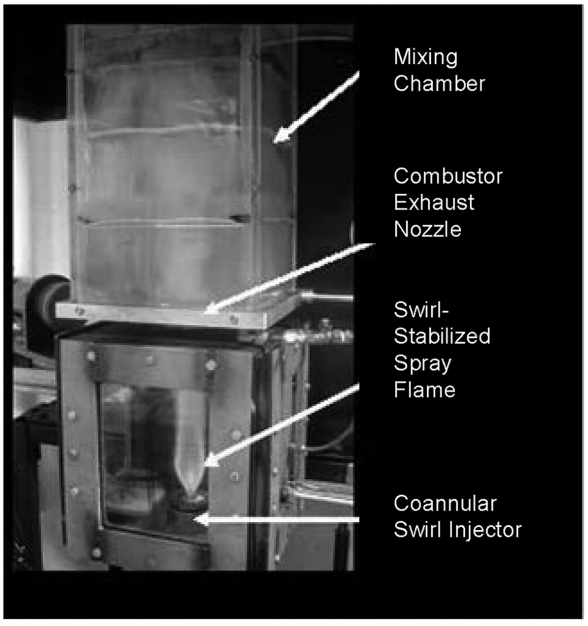

Fig. 2 Submerged combustor in operation.

The completed test section is shown in Fig. 2. The mixing chamber was equipped with a baffle cartridge, which allowed high-speed exhaust jets to be examined in a compact experimental system. The entire system was built on a positioning stage, allowing the test section to be moved in three dimensions with great precision.

The interaction of the exhaust gases from the combustion chamber with water in the mixing chamber caused two-phase shear-layer interaction between exhaust gases and the water in the downstream mixing chamber. In general, if the combustor pressure in a submerged combustor is only slightly higher than the ambient pressure, the submerged condition will have an impact on the shear-layer mixing between the two fluid streams and may cause a subsequent effect on combustor performance. If the combustor is at a significantly higher pressure than the ambient pressure, the flow becomes choked to effectively decouple conditions in the combustor from those downstream of the exhaust nozzle. Work was carried out to examine the behavior of submerged exhaust jets under conditions relevant to unchoked and choked exhaust flows under submerged conditions.

II. Experimental Equipment

A schematic of the combustor section is shown in Fig. 3. The combustor had a square cross section, with a diameter expansion ratio of 3.91. Quartz windows, 12.5 mm thick, were positioned on three of the sides. The fourth side was a steel plate and had ports that allowed probes, igniters, or pressure taps to be installed. The

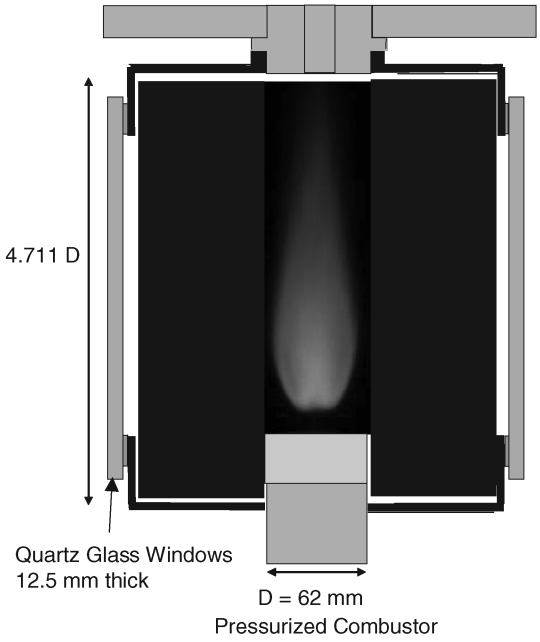

Fig. 3 Schematic diagram of the combustor section.

combustor exit had the same outer diameter as the inlet. A nozzle block could be installed in the outlet to constrict the flow. The nozzle block was aluminum and was fitted with stainless steel nozzles of different geometries. Thus, a variety of the combustor pressures and exhaust nozzle geometries were investigated using the same combustor mass flow rate and heat release.

The injector featured coannular air passages surrounding a central fuel nozzle. The fuel nozzle was an air-assisted atomizing system; however, a variety of atomizing gases have been employed in previous investigations. Each air annulus could be fitted with a swirl vane assembly, allowing the swirl strength and flow distribution through the inner and outer annuli to be varied. A schematic of the injector is shown in Fig. 4.

The inner swirler used in the current investigation was a helical-vane swirler. The helical-vane swirler design facilitated analysis of the swirl condition at the burner inlet. The swirl angle of the outer edge of the vanes on the inner swirler was 45 deg, creating a swirl number S of approximately 0.7. The outer swirler was a straight-vane swirler assembly, with a swirl angle of 0 deg. In this case, the swirl configuration will be referred to as a 45-i/null-o swirl configuration.

The fuel spray nozzle has been found (in previous investigations) to create a fuel spray with a mean diameter near 50 μm [5]. In the current investigation, the nozzle formed a solid-cone spray, with the fuel also distributed near the centerline of the spray. High-purity methanol was used as the test fuel, largely to avoid soot buildup on the combustor windows and simplify analysis of the combustion chemistry. The combustion and atomization-airflow rates were measured using high-precision orifices and pressure gauges. The fuel flow rate was measured using a digital turbine flowmeter.

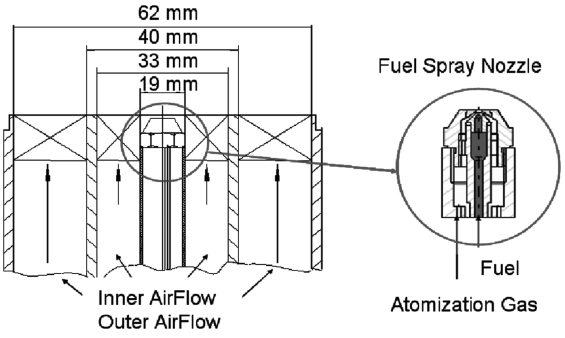

Fig. 4 Schematic diagram of the combustor section.

A. Mixing Chamber

The base of the mixing chamber was an aluminum base plate, 1 in. thick, equipped with slots into which the walls could be set. The walls were made of transparent acrylic sheets and were screwed together so that the walls supported themselves with no support frame. A nylon lid, also 1 in. thick and slotted, enclosed the top of the chamber. Four exhaust ports equipped with stainless steel trap stacks were cut through the lid for the exhaust gases to escape. The horizontal cross section of the chamber was square, and the dimensions of the chamber are shown in Fig. 5.

The exhaust jet tended to entrain water and to expel this water from the top of the tank. The jet also violently agitated the water, and this caused large-scale sloshing of water in the chamber. This sloshing was quite problematic, in that it caused the entire experimental facility to rock violently back and forth if it remained uncontrolled. In addition, high-velocity exhaust jets, with average velocities on the order of hundreds of m/s, were found to produce very small bubbles, with diameters on the order of 10–100 μm. These bubbles recirculated in the water, completely obscuring the exhaust jet and making optical examination of the jet impossible. To examine jets with average velocities on the order of 400 m/s, it was necessary to control the large-scale motion of the fluid in the mixing chamber, as well as these small bubbles, without compromising optical access and without interfering in the development of unstable interactions between the exhaust jet and water near the exhaust port.

To this end, a four-stage baffle cartridge was developed. No particular theory was applied during the design, but the approach was similar to that employed in fuel tanks for liquid-fueled rockets. Designs were tested iteratively until a satisfactory arrangement was obtained. It was found that a four-stage approach separated the chamber into three separate recirculation zones in which the vapor was effectively separated from the liquid.

The resulting baffle cartridge is shown in Fig. 5. The baffles were made of perforated aluminum with a 33% porosity ratio and were attached to the lid via aluminum struts. A wide hole was cut through the lowest baffle plate to allow the exhaust jet to pass through with very little interference. The purpose of this plate was to interfere with very small bubbles, which tended to travel down along the walls. This plate caught the bubbles and prevented them from traveling all the way down the walls, where they would interfere with observation of the exhaust jet.

The second plate had a smaller hole cut through the center. The purpose of this hole was to allow the vapor core of the exhaust jet to pass while restricting the passage of entrained liquid at the edges of the jet. Finally, the last two baffle plates were designed to trap any remaining entrained liquid.

The trap stacks on top of the lid were also fitted with internal wire screens, which effectively trapped mist and fine droplets. It was found that once the proper baffle design had been developed, exhaust jets with average velocities up to 400 m/s could be effectively observed in the mixing chamber. The trap system was so effective that the amount of liquid escaping from the mixing chamber was negligible: only the finest mist, entrained in the exhaust stream from the trap stacks, was observed.

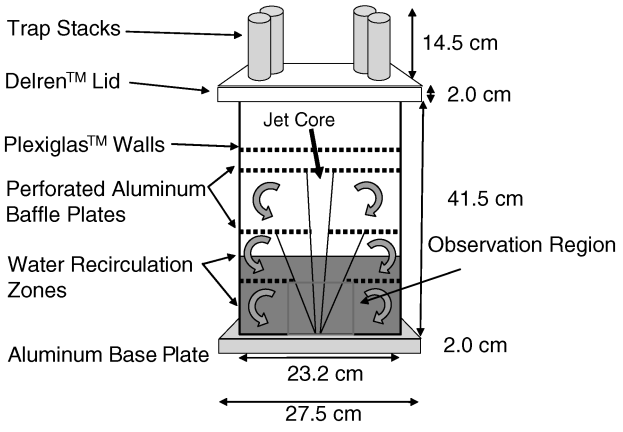

Fig. 5 Schematic diagram of the mixing chamber.

B. Exhaust Nozzles

Considerable work has been done on the development of turbulent interactions between jets and surrounding fluid in single-phase situations. The interface between the fast-moving jet and the stationary ambient fluid has been found to develop Kelvin–Helmholtz instabilities (KHI), and the resulting turbulent structures have been found to display certain characteristic Strouhal numbers [6]. The Strouhal number St of an instability is given by

$$St \equiv \frac{f \times L}{V} \tag{1}$$

The Strouhal number nondimensionalizes the frequency f of an event occurring in the flow using the characteristic length L and the mean flow velocity V. In single-phase systems, it has been found that the geometry of the exhaust nozzle may have a significant effect on the unstable behavior of these flows. Changes in the radius of curvature along the nozzle wall, which produce turbulent structures of different length scales at the interface, have been shown to assist in mixing between the fluid in the jet and the surrounding material [7]. These changes in nozzle geometry can change the Strouhal number of turbulent structures developed at the jet boundary, which affects mixing and noise emission associated with these flows.

Less is known about jet interaction in a two-phase environment. The presence of a two-phase interface and the incompressibility of a liquid phase, as well as the presence of significant buoyant forces, make the behavior of the interaction much more difficult to predict or characterize. In high-speed flows, in which a sonic condition may be present in the nozzle, pressure-wave interactions at the interface may also play a role.

To shed some light on these issues, three exhaust nozzles were developed. Each was cut from type 304 stainless steel and was fitted with an O-ring to provide an effective seal. The flush-mounted nozzle (FMN), conical projecting nozzle (CPN), and corrugated converging–diverging nozzle (CCDN) are shown in Fig. 6.

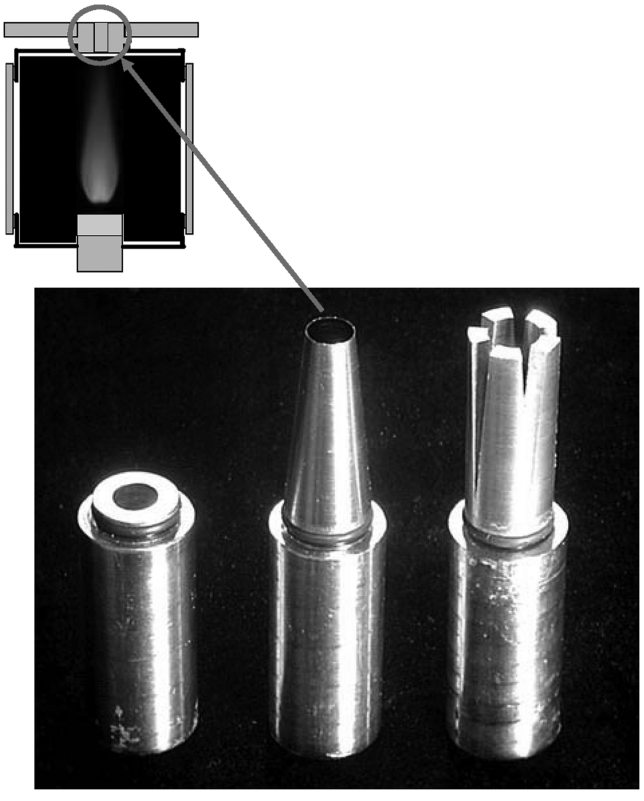

Fig. 6 FMN (left), CPN (center), and CCDN (right) exhaust nozzles.

1. Flush-Mounted Nozzle

The FMN was a simple flush-mounted design. The dimensions of the nozzle are shown in the schematic in Fig. 7. In this nozzle, the flow was constricted in the throat, and the downstream lip of the nozzle was mounted flush with the face of the mixing-chamber base plate. No attempt was made in this design to modify the behavior of the jet or two-phase interface in any particular way.

2. Conical Projecting Nozzle

The CPN projected 40.64 mm above the level of the base plate and tapered in a conical fashion to the final jet diameter of 8.71 mm. The nozzle is shown schematically in Fig. 8. The objective in this case was to compare the projecting nozzle with the flush-mounted nozzle and to observe any changes in the behavior of the interface caused by the changed geometry.

3. Corrugated Converging–Diverging Nozzle

The CCDN was designed to produce a fully expanded or overexpanded jet for any throat Mach number conditions up to Mach 1.5. Shown schematically in Fig. 9, the nozzle projected 40.64 mm above the base plate, as in the case of the conical projecting nozzle. The flow was constricted, just as in the case of the other two nozzles, but in this case, the duct area was then expanded by 20%. The projecting walls of the nozzle were also shaped to apply some of the more advanced techniques for control of jet instabilities described by other authors [7,8]. Five corrugated tapering slots were cut into the walls of the nozzle; these can be seen in detail in Fig. 10. The corrugations were cut in such a way that the wall of the combustor was perforated; this allowed the jet to interact with the liquid at a number of points and along an interface with many local radii of curvature. In single-phase systems, this approach has been shown to change the length scales of the mixing interaction between the fast-moving jet and the surrounding fluid, and the objective of the CCDN design was to examine the effect of these nozzle features in a two-phase interaction situation.

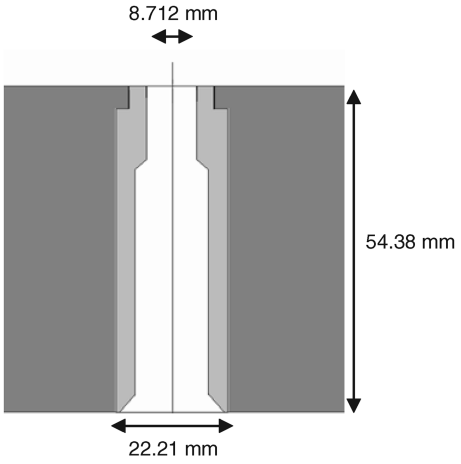

Fig. 7 FMN schematic.

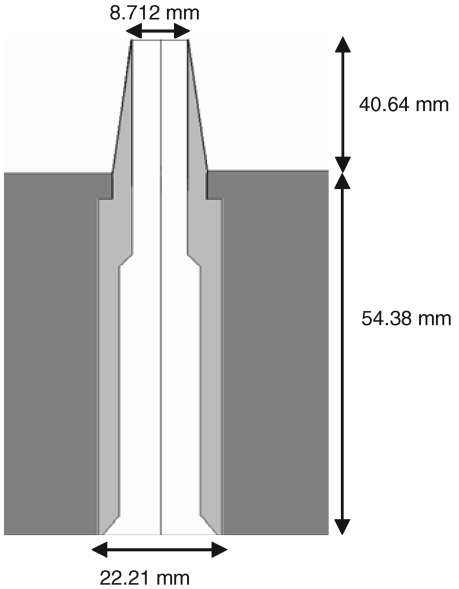

Fig. 8 CPN schematic.

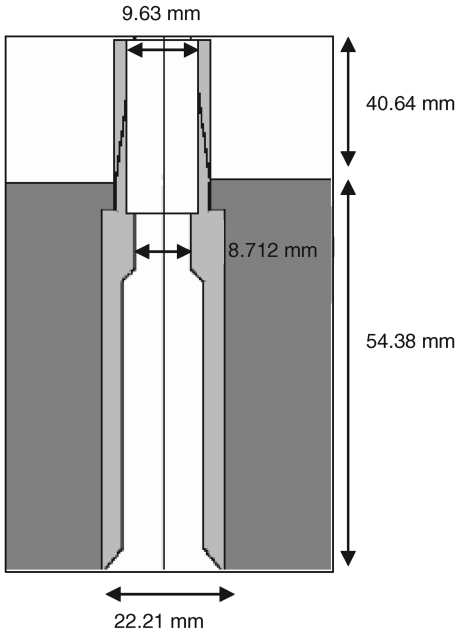

Fig. 9 CCDN schematic.

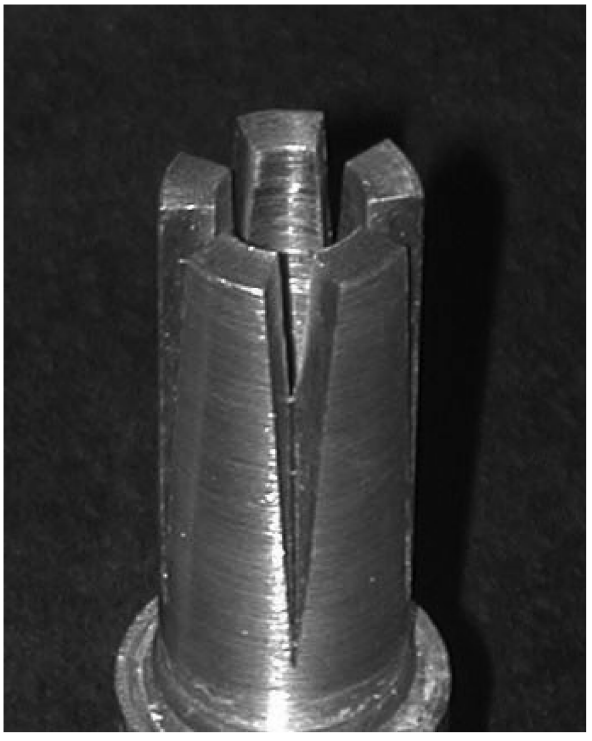

Fig. 10 Detail of CCDN, showing corrugations and perforations through nozzle wall.

III. Underwater-Propulsion Studies

A. Submerged Nonreacting Experiments

To examine the combustor under submerged conditions, the mixing chamber (with its baffle cartridge) and exhaust nozzles were installed. A small airflow rate was fed to the combustor, so that the pressure in the combustor was 0.4 psig higher than the ambient. Once the combustor pressure was slightly elevated, the mixing chamber was filled with water to a depth of 15 cm. The lowest baffle plate was submerged when the mixing chamber was filled to this level. Air emerged continuously from the exhaust nozzle during filling, preventing any water from entering the combustor.

A stream of air was then fed into the combustor until the combustor pressure rose to 1 psig (total pressure 1.07 bar). The combustor pressure P_C was found to be the most important parameter affecting the behavior of the exhaust jet. Swirl associated with the air was found to play no role in determining the exhaust jet behavior. The entire stream of air fed into the combustor could be fed through either the inner annulus, in which it acquired swirl, or through the outer annulus, in which it acquired no swirl, without affecting the two-phase interaction of the exhaust stream.

1. *Unchoked Flow*

With $P_C = 1.07$ bar, the exhaust jet was observed to emerge from all three exhaust nozzles as a repeatable series of bubbles, for which the motion depended primarily on buoyancy forces. Images of the exhaust jet were recorded at 500 frames per second. Stills showing a representative bubble cycle produced by each of the three nozzles (FMN, CPN, and CCDN) are shown in Figs. 11–13. Significantly, the nozzle geometry at this combustor pressure had very little effect on the shape of the bubbles emerging from the nozzle and it did not greatly affect the frequency with which the bubbles emerged.

The Strouhal numbers of the bubble-formation cycles were calculated for each nozzle geometry using Eq. (1). Some variation in the duration of the cycle was observed, and the Strouhal numbers reported for each geometry are average values. The Strouhal number of the bubble-emergence cycle for the flush-mounted nozzle was found to be 0.0023. When the CPN nozzle was used, the Strouhal number of the bubble-formation cycle was found to be 0.0037, and when the CCDN nozzle was used, the Strouhal number was 0.0045. These values are much smaller than those associated with shear-layer instabilities in single-phase flows, in which the Strouhal number is usually found to be 0.2 to 0.5 [6]. The Strouhal numbers varied slightly with nozzle geometry, because the shape of the trailing edge of the bubble was different. In a buoyancy-driven flow, the rate at which a bubble of gas can rise through the surrounding liquid depends on the balance between buoyant forces and drag forces acting on the bubble. The bubbles formed by the projecting nozzles (CPN and CCDN) were immediately able to form smoothly rounded trailing edges, which allowed them to rise more rapidly. The lower surface of the bubbles emerging from the CCDN nozzle was initially distorted by lobe-shaped structures emerging from the perforations in the nozzle. This effect is shown in Fig. 14. However, as the bubble emerged fully, the lobe-shaped distortions disappeared, due to surface tension, allowing a smoothly rounded lower surface to form on each bubble. The flow emerging from the FMN initially spread out laterally before rising to form the bubble, and the formation of the lower portion of the interface took more time. As a result, the Strouhal number was lower.

The total diameter achieved by the bubbles was consistently approximately $5D_E$, where D_E was the diameter of the throat of the exhaust nozzle.

2. *Choked Flow*

Further nonreacting experiments were carried out with airflows emerging from the combustor with $P_C = 2.02$ bar. In this case, the flow through the exhaust nozzles was choked, because the necessary pressure drop across the exhaust nozzle was present. The agitation of the water in the mixing chamber was much more violent at the higher pressure condition, and direct observation of the behavior of the

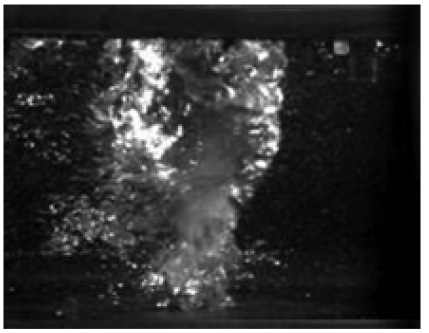

a) Phase angle: 0 deg

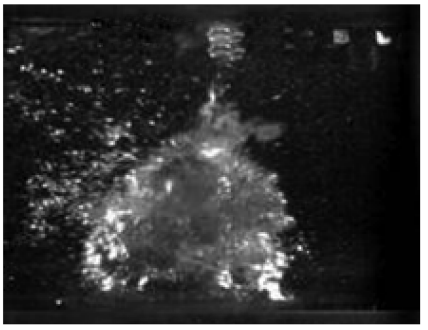

b) Phase angle: 90 deg

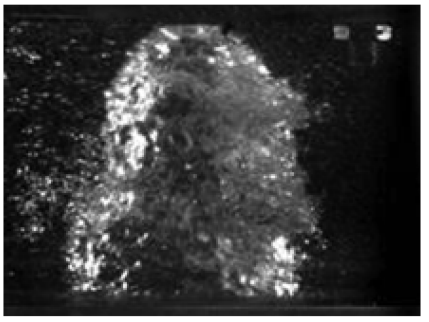

c) Phase angle: 180 deg

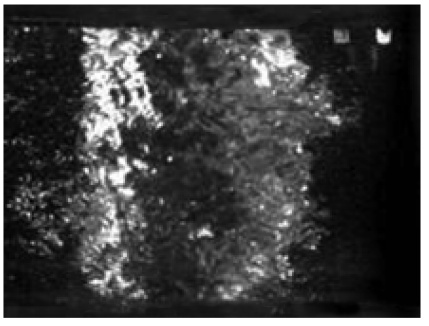

d) Phase angle: 270 deg

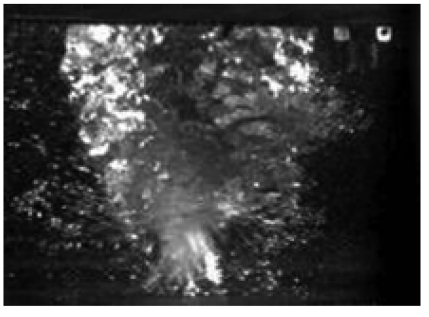

e) Phase angle: 0 deg

Fig. 11 Bubble-emergence cycle, flush-mounted nozzle.

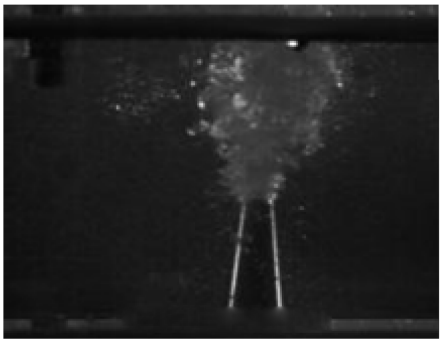

a) Phase angle: 0 deg

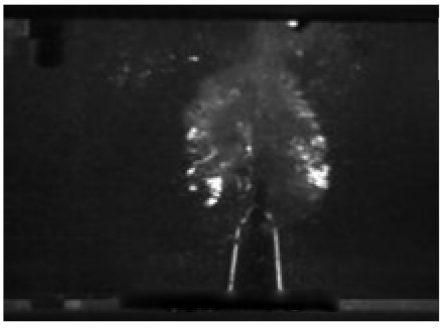

b) Phase angle: 90 deg

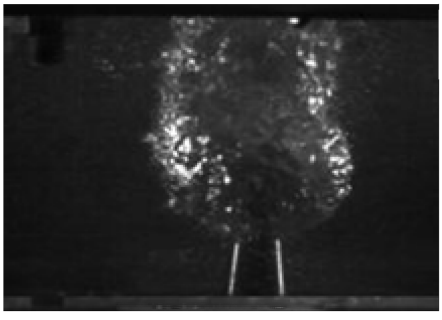

c) Phase angle: 180 deg

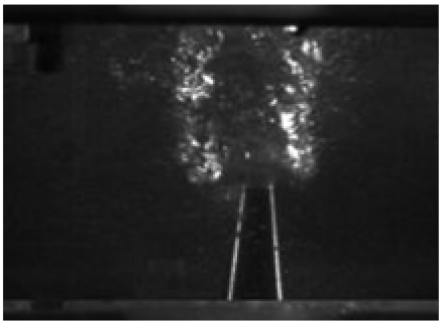

d) Phase angle: 270 deg

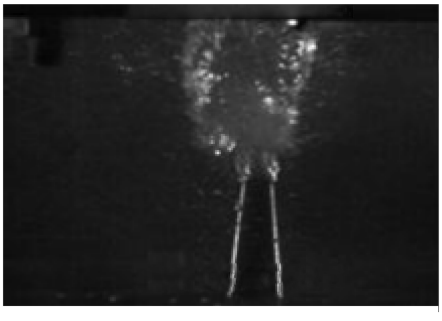

e) Phase angle: 0 deg

Fig. 12 Bubble-emergence cycle, conical projecting nozzle.

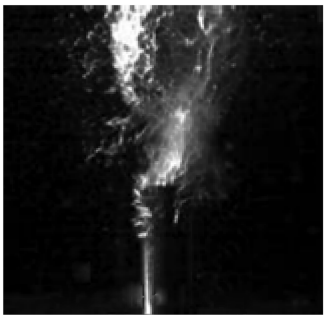

a) Phase angle: 0 deg

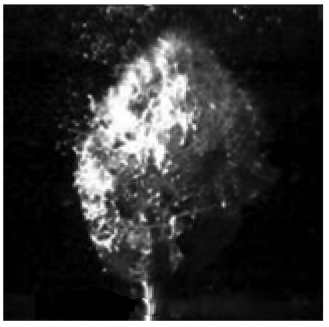

b) Phase angle: 90 deg

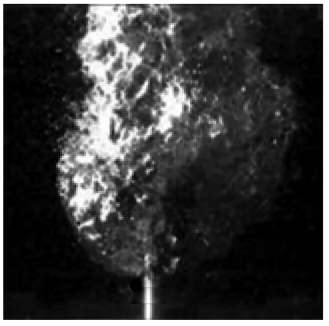

c) Phase angle: 180 deg

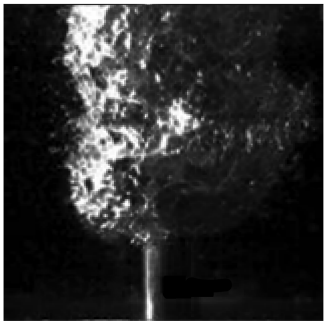

d) Phase angle: 270 deg

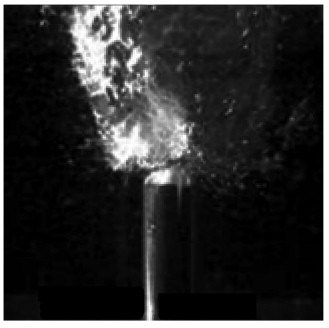

e) Phase angle: 0 deg

Fig. 13 Bubble-emergence cycle, corrugated converging–diverging nozzle.

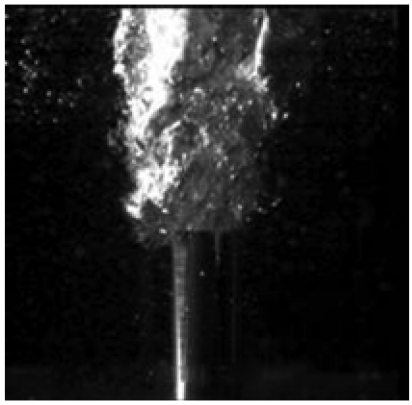

a) Phase angle: 0 deg

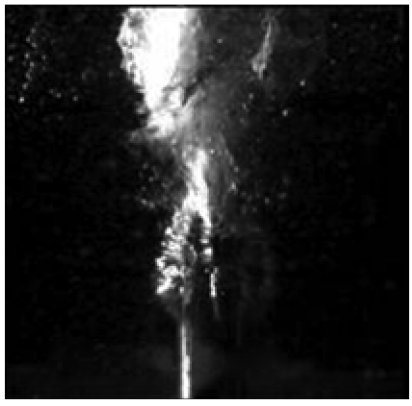

b) Phase angle: 30 deg

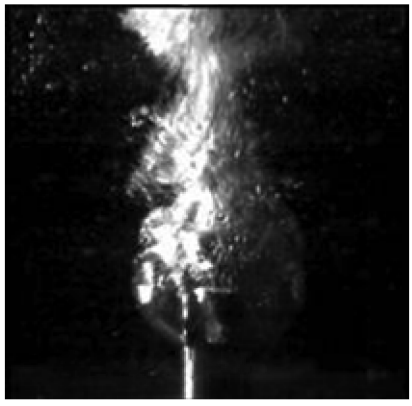

c) Phase angle: 60 deg

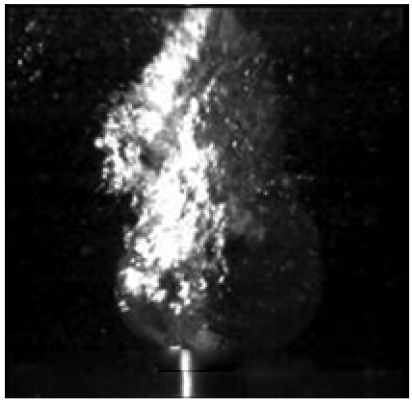

d) Phase angle: 90 deg

Fig. 14 Initial phase of bubble emergence from the CCDN nozzle, showing lobe-shaped distortions of bubble surface due to ejections from perforations.

exhaust jet emerging from the FMN was impossible. The water rapidly became so clouded by small bubbles that the region in the vicinity of the exhaust jet was obscured.

However, the exhaust jet emerging from the pressurized combustor could be observed if either the CPN or CCDN were installed. Two general jet modes were observed at this combustor pressure condition. The first mode, which will be referred to as an open-jet mode, consisted of an open channel to the surface of the water. The walls of the channel angled outward at approximately 30 deg. This jet mode seen emerging from the CPN nozzle is shown in Fig. 15. The open-jet mode was not stable, however, and collapsed occasionally, at apparently random intervals. When such a collapse occurred, the nozzle was briefly blocked by water. A round bubble then formed around the nozzle, with a heavily corrugated surface. The bubble rapidly disintegrated into a cloud of much smaller bubbles, a few millimeters in diameter. Interestingly, the maximum diameter reached by the bubble structure in this mode was still $5D_E$, just as had been the case at the lower combustor pressure. Multiple bubble structures sometimes occurred in close succession before the open-jet mode could be reestablished. The Strouhal number of this cycle was also found to be approximately 0.002 to 0.005. This jet mode will be referred to as the bubble-formation mode. An image of such a bubble emerging from the CPN nozzle at its maximum diameter just before breakup is shown in Fig. 16.

The open-jet and bubble-formation modes were observed for both the CPN and CCDN nozzles. The type of unstable cycle and the mechanism of open-jet formation and collapse did not appear to be effectively controlled by the special features built into the CCDN nozzle. However, the perforations cut through the walls of the CCDN nozzle did allow gas to escape further upstream, closer to the mixing-chamber base plate, when this nozzle was used. The perforations also produced a more heavily corrugated surface in the air/water interface,

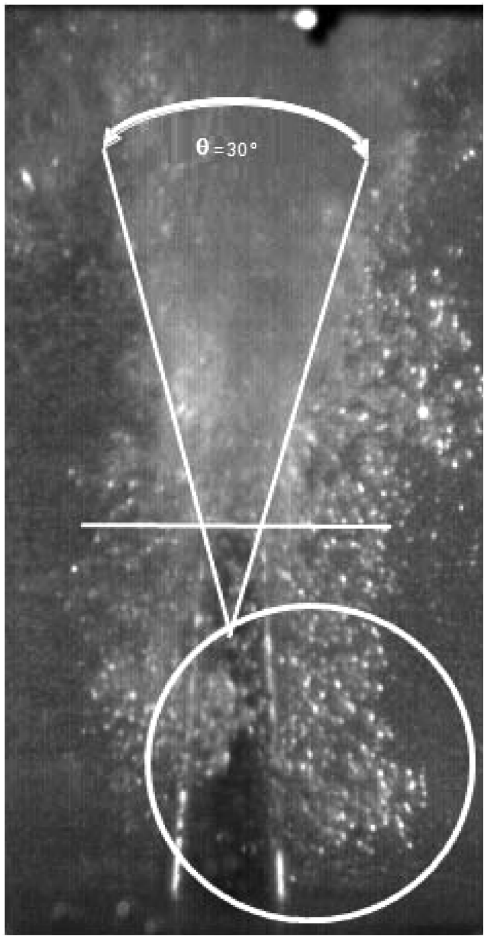

Fig. 15 Open-jet mode, observed at $P_C = 2.02$ bar; bubbles ejected upstream are circled.

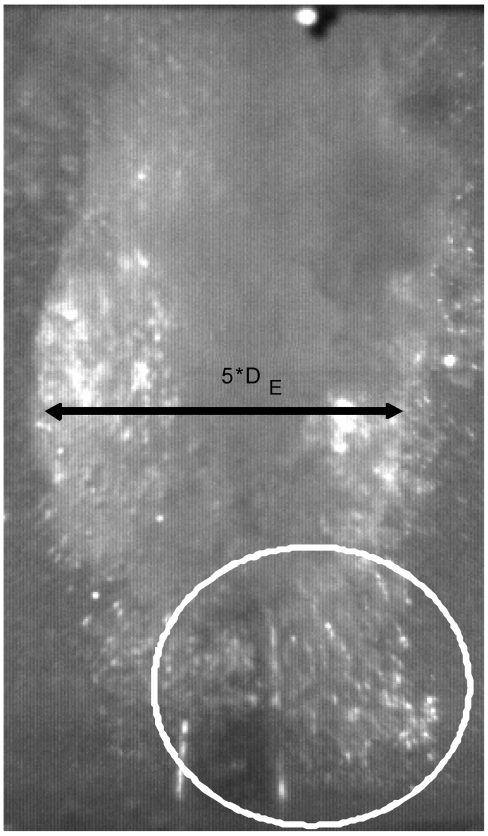

Fig. 16 Bubble mode, observed at $P_C = 2.02$ bar; bubbles ejected upstream are circled.

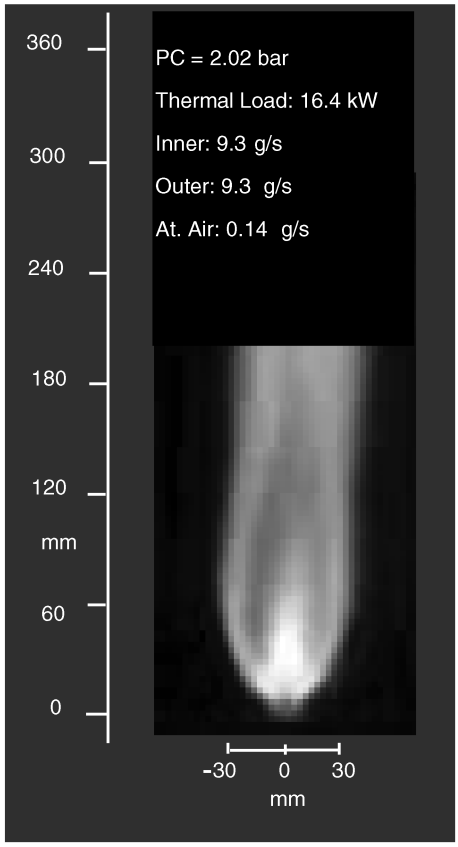

Fig. 17 Pressurized, submerged flame.

because lobe-shaped gas structures were forced laterally out of the nozzle through the perforations.

One further observation was made. The high-speed jets were generally surrounded by veils of small bubbles, with diameters on the order of millimeters. These bubbles are indicated by the circled regions in Figs. 15 and 16. These bubbles were often ejected upstream, toward the base plate, and then slowly rose upward due to buoyancy. The mechanism by which these bubbles were formed may be indicative of particular instability mechanisms present in the two-phase regime. In particular, pressure fluctuations interacting with the interface may play a role in the creation and location of these bubbles. The possible nature of the instability mechanism is discussed in greater detail in the Discussion section. No comparable behavior has ever been reported in single-phase systems. Neither the momentum of the exhaust jet nor the buoyancy would appear to explain their presence in the regions in which they are observed, and so the process by which these bubbles are formed will be discussed in greater detail in the Discussion section.

B. Submerged Reacting Flow

A submerged flame venting its exhaust jet into the mixing chamber can be seen in Fig. 2. The flame shown in the image is a preliminary trial flame; the flame geometry shown differs slightly from the final flame achieved at the correct experimental conditions. The flow in the mixing chamber in the image is a white blur; the exposure duration used for the photograph was too long to capture the detailed motion of the two-phase flow.

To examine the behavior of the two-phase interaction of an exhaust jet produced by a reacting flow, a 16.4 kW flame, using 9.3 g/s of air through both the inner and outer annuli, 0.14 g/s of atomization air, and the 45-i/null-o swirl configuration, was created under submerged conditions. The combustor pressure in this case rose to 2.02 bar. An image of this flame is shown in Fig. 17.

The exhaust jet associated with this flame was forced out through both the CPN and CCDN nozzles, and the two-phase interaction was examined. Images of each condition are shown in Fig. 18. The exhaust jets produced by the flame in the combustor were extremely chaotic. Dynamic events occurring in a wide range of timescales distorted and interrupted the structure of the flow. Both flows were also completely engulfed in curtains of small bubbles, which were again often ejected outward and downward. The distance traveled by the bubbles was greater in this case in which combustion was present than it would have been in the case of the nonreacting flow at the same P_C value. This observation is again consistent with pressure-wave driven instability, and this effect will be discussed further subsequently.

The absence of a dramatic difference between the jet properties observed with the CPN and CCDN nozzles under nonreacting and reacting flow conditions is also an indication that the flow in the two-phase regime is affected by fundamentally different instability mechanisms than are present in single-phase jet interaction. This point will also be discussed in further detail in the Discussion section.

C. Sound Spectrum Analysis

The experimental diagnostics available for examination of a two-phase system such as that in the mixing chamber are limited. However, sound spectrum analysis represents a way to generate detailed information on the dynamic events occurring in the flow. A sound spectrum analyzer was connected to the base plate of the mixing chamber, and sound spectra associated with the CPN and CCDN nozzles were obtained. Nonreacting cases at $P_C = 1.07$ and 2.02 bar were examined. The effect of the combustion on the sound spectrum of the exhaust jet leaving the CCDN nozzle was also examined. The sound spectrum produced by the jet from the 16.4 kW flame at $P_C = 2.02$ bar was compared with the spectrum of the nonreacting air jet at the same combustor pressure.

The effect of increased combustor pressure on the CPN and CCDN sound spectra is shown in Figs. 19 and 20. The principal effect of increased combustor pressure was seen at frequencies above 50 Hz. The lowest frequencies in the spectrum, which likely corresponded to unstable events in the jet with the largest length scales, were almost

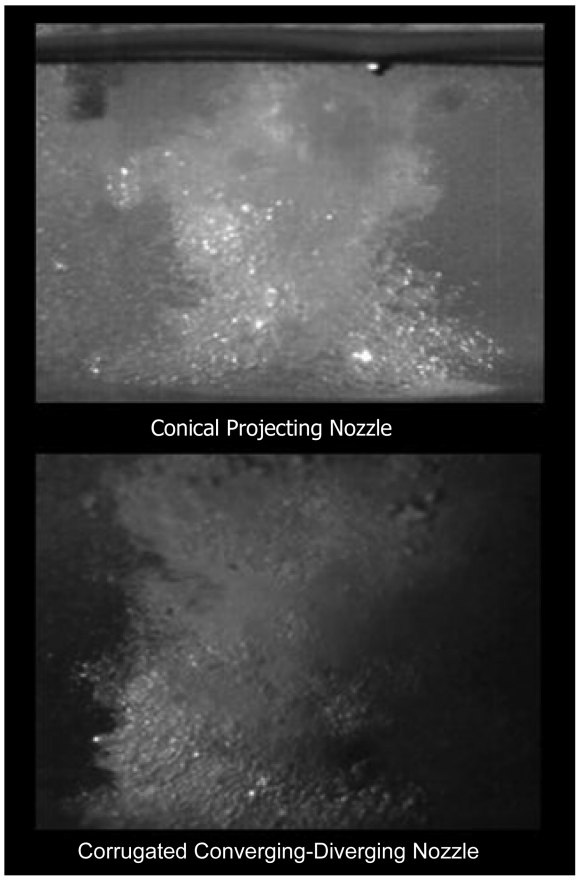

Fig. 18 Exhaust jets produced by reacting flow in the combustor with $P_C = 2.02$ bar; note curtains of bubbles surrounding jets from both CPN and CCDN nozzles.

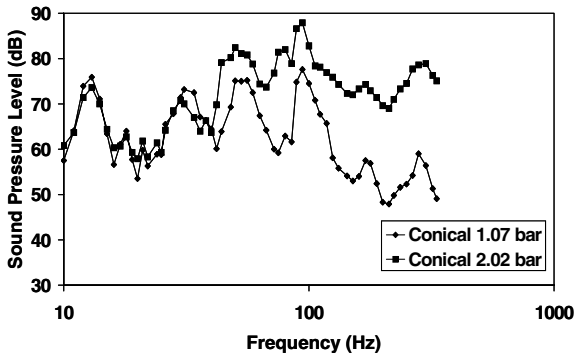

Fig. 19 Sound spectra associated with the CPN nozzle, nonreacting flow, showing the effect of increased pressure.

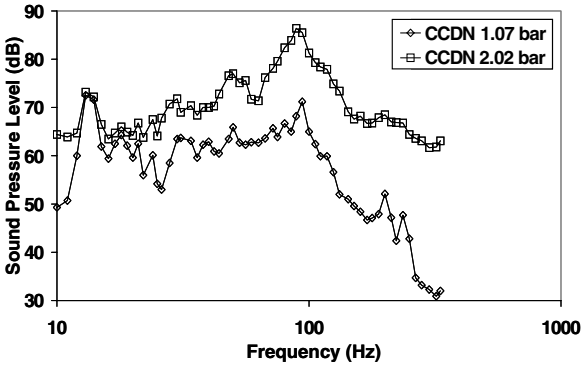

Fig. 20 Sound spectra associated with the CCDN nozzle; nonreacting flow, showing the effect of increased pressure.

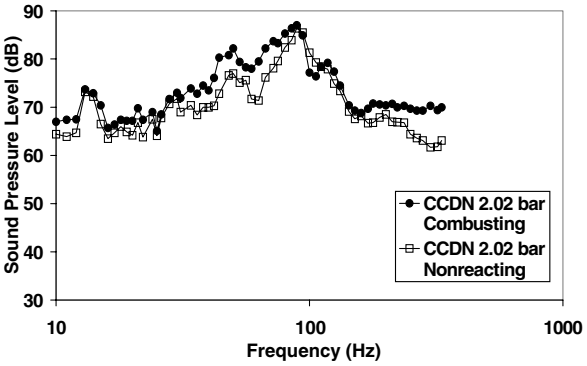

Fig. 21 Sound spectra associated with the CCDN nozzle showing the effect of the combustion.

unaffected. The sound pressure levels associated with the higher frequencies (near 300 Hz) were increased by up to 20 dB.

Although there were some differences in the sound spectra obtained for the CPN and CCDN nozzles, important features of the spectra were not affected by the changes in nozzle geometry. Both nozzles had associated sound spectra with local maxima at approximately 20 and 100 Hz. Other areas of the spectrum displayed differences, implying that some limited effect on the sound spectrum and on the dynamic behavior of the flow can be achieved through changes in exhaust nozzle geometry.

The effect of the combustion (as compared with the nonreacting airflow) on the sound spectrum of the jet emerging from the CCDN nozzle was also limited and is shown in Fig. 21. Interestingly, the shape of the curve was nearly identical in the combusting and noncombusting cases. At most frequencies, the reacting flow displayed sound pressures 2–5 dB greater than the nonreacting flow. The added energy from the flame may be responsible for this effect. Other factors, such as the effect of increased temperature on the viscosity of the liquid phase, may also play a role.

The trends shown by the sound spectra are particularly important when considered in connection with the observed behavior of the interface and the ejection of small bubbles through the interface.

IV. Discussion

The interface between the exhaust jet and the liquid phase in the mixing chamber is clearly affected by instability mechanisms not seen in single-phase systems. When the combustor pressure was increased to 2.02 bar under nonreacting airflow-only conditions, the dynamics affecting the exhaust jet were seen to change. The regular emission of distinct bubbles was not observed; instead, the exhaust jet displayed unstable behavior in a wide range of temporal and spatial scales. A detailed description of the unstable behavior of the jet is not possible at this point, due to the complexity of the instabilities observed and the complications introduced by the two-phase interface between the exhaust gas jet and water.

Given that both CPN and CCDN nozzles display very similar dynamic behavior, it seems clear that the dynamics affecting two-phase interaction are fundamentally different from those affecting single-phase jet interactions. The jet was also surrounded much of the time by curtains of small bubbles that were ejected outward from the exhaust jet to maximum distances anywhere from $2D_E$ to $10D_E$. The mechanism by which these bubble curtains were generated may indicate the presence of an instability mechanism similar to Richtmyer–Meshkov instability (RMI).

The RMI mechanism has been studied in a number of contexts, including the evolution of structures in stellar nebulas and laser-driven nuclear fusion experiments. Essentially, RMI occurs when a shock wave travels through one phase and collides with a phase interface [9]. In systems in which RMI has been examined, the shock originates in the denser of the two phases. A rarefaction wave is reflected from the interface back through the phase in which the shock wave originated, and the interface itself is distorted and pushed forward through the adjacent phase as the shock wave passes

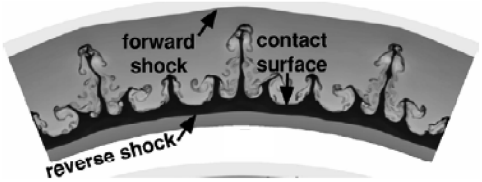

Fig. 22 Interface distortion via RMI (from Drake [10]).

through. The growth of the distortion in the interface is initially linear, but rapidly becomes nonlinear past a certain point. Once an interface distortion has been amplified far enough, the boundaries of the distortion are themselves affected by KHI, which distorts the boundary and produces a distinct mushroom-shaped structure. The boundary will then tend to be further affected by turbulence. This effect is shown directly in Fig. 22 (from Drake [10]). Drake investigated RMI in connection with shock interactions between adjacent regions in stellar nebulas. The effect of RMI on structures seen in supernovas is also examined by Kane et al. [11]. However, the same type of mechanism, driven by weaker acoustic pressure fluctuations, may be connected with the clouds of bubbles that surround the exhaust jet emerging from the submerged combustor. A jet of gas punched through the interface by a shock wave can remain a coherent jet only briefly. It must break down rapidly into a string of bubbles, which are then controlled by surface tension, drag, and buoyancy. This mechanism may explain how clouds of bubbles are generated upstream of the exhaust nozzle exit and the fact that the bubbles associated with the exhaust jet from the combusting case penetrate further into the surrounding liquid.

The effect of the combustion on the observed unstable behavior of the exhaust jet in the experiments described earlier offers further evidence that pressure waves may play an important role in determining the exhaust jet behavior. In the combusting cases, the clouds of small bubbles ejected by the jet were seen to be denser, and the bubbles were ejected further from the jet. This is consistent with the sound spectra of the jet, which shows somewhat higher sound pressure levels at almost every frequency, including the peak at 100 Hz. The effect of the combustion appears to promote the lateral ejection of bubbles, partly because amplitudes of sound pressure waves are increased and perhaps also because the viscosity of water in the immediate vicinity of the jet is reduced by the heated exhaust stream.

There are several further factors that make a straightforward analysis of this phenomenon difficult. First, RMI is usually studied in connection with large-amplitude shock waves. In the two-phase exhaust jets examined here, there is no evidence of a direct interaction between a shock wave and the interface; any pressure-wave-induced distortion of the interface must take place in connection with acoustic pressure waves. RMI is generally encountered in systems in which an acceleration of both phases is oriented coaxially with the path of the pressure wave. In the two-phase exhaust jets, the interface is vertical (rather than horizontal) and the acceleration due to gravity, as well as the gradient in density between phases, is not necessarily aligned with the path of the wave. RMI is also generally associated with systems in which the pressure wave travels through the more dense phase and rebounds from the interface between the more dense and less dense phases. The denser phase is driven effectively into the less dense phase. In the exhaust jet instability described here, however, an acoustic wave would have to push the less dense (gas) phase into the more dense (liquid) phase to produce bubbles located at great distances from the exhaust jet. Some question exists, therefore, as to whether a pressure-wave interaction of the type proposed here would really be RMI or whether it would be an example of a less specific type of baroclinic instability. Baroclinic instability associated with the passage of vortices through flame fronts is discussed by Mueller et al. [12]. Their description of the effects of misalignments between the density vectors and pressure vectors in jets may be relevant to two-phase systems of the type discussed in the present work. A similar baroclinic effect is described by Sinibaldi et al. [13].

Further, the increase in the number of bubbles associated with the heated jet may be due to the increased exhaust jet temperature, rather than an increase in the amplitudes of frequencies in the sound spectrum. Although the bulk temperature of the water phase never exceeded 40°C in these trials, liquid water may be vaporizing at the interface, destabilizing it, and promoting the ejection of bubbles. Bubbles may also be forming near the interface and then being pushed outward by large-scale motions of the liquid phase, which cannot be characterized directly in the present experiments. Further investigation into these phenomena could yield fundamental insights into the precise nature of the instabilities affecting these kinds of interfaces.

V. Conclusions

Three nozzle geometries were compared, and the impact of nozzle geometry on the two-phase jet interaction was assessed. The two-phase interaction of the exhaust jet was found to depend heavily on the pressure drop over the exhaust nozzle. The dynamic behavior of the exhaust jet was buoyancy-driven at low-pressure drops and was affected by complex instability mechanisms at high-pressure drops. Nozzle features that have been shown to affect the unstable behavior of single-phase jet shear-layer instability are found to have little effect in a two-phase situation. The instability mechanisms involved in the two-phase cases investigated here are shown to be significantly different from those affecting jets in single-phase cases. A pressure-wave instability mechanism may be responsible for certain phenomena observed in the two-phase interaction: particularly, clouds of small bubbles seen to surround the exhaust jet when the combustor pressure was high and when the exhaust jet was heated and emerged from a combustor in which a flame was present.

Acknowledgment

The work presented here has been carried out with the support and assistance of the Office of Naval Research (ONR) Propulsion Group (director Gabriel Roy). The support of this organization is gratefully acknowledged.

References

[1] Linck, M., Gupta, A. K., Bourhis, G., and Yu, K., "Combustion Characteristics of Pressurized Swirling Spray Flame and Unsteady Two-Phase Exhaust Jet," 44th AIAA Aerospace Sciences Meeting and Exhibit, Reno, NV, AIAA Paper 2006-0377, Jan. 2006.

[2] Linck, M., Armani, M., and Gupta, A. K., "Passive Control of Unstable Combustion in a Swirl-Stabilized Spray Combustor," 42nd Aerospace Sciences Meeting and Exhibit, Reno, NV, AIAA Paper 2004-8010, Jan. 2004.

[3] Linck, M., Armani, M., and, A. K., Gupta, A. K., "Effect of Swirl and Fuel Pulsation on Flame Dynamics, Flame Structure, and Droplet Dynamics in Swirl Stabilized Spray Flames," ASME Power Conference, Baltimore, MD, American Society of Mechanical Engineers Paper 2004-52048, 2004.

[4] Gupta, A. K., Lilley, D. G., and Syred, N., *Swirl Flows*, Abacus Press, Cambridge, MA, 1984.

[5] Linck, M., and Gupta, A. K., "Effect of Swirl and Combustion on Flow Dynamics in Luminous Kerosene Spray Flames," 41st AIAA Aerospace Sciences Meeting and Exhibit, Reno, NV, AIAA Paper 2003-1345, Jan. 2003.

[6] Schadow, K. C., and Gutmark, E., "Combustion Instability Related to Vortex Shedding in Dump Combustors and their Passive Control," *Progress in Energy and Combustion Science*, Vol. 18, No. 2, 1992, pp. 117–131. doi:10.1016/0360-1285(92)90020-2

[7] Gutmark, E. J., Grinstein, F. F., "Flow Control With Noncircular Jets," *Annual Review of Fluid Mechanics*, Vol. 31, 1999, pp. 239–272. doi:10.1146/annurev.fluid.31.1.239

[8] Hu, H., Saga, T., Kobayashi, T., Taniguchi, N., "Passive Control on Jet Mixing Flows by using Vortex Generators," *6th Triennial Symposium on Fluid Control*, Sherbrooke, Canada, Aug. 2000.

[9] Brouillette, M., "The Richtmyer–Meshkov Instability," *Annual Review of Fluid Mechanics*, Vol. 34, 2002, pp. 445–468. doi:10.1146/annurev.fluid.34.090101.162238

[10] Drake, R. P., "Hydrodynamic Instabilities in Astrophysics and in

Laboratory High-Energy-Density Systems," *Plasma Physics and Controlled Fusion*, Vol. 47, 2005, pp. B419–B440.
doi:10.1088/0741-3335/47/12B/S30

[11] Kane, J., Drake, R. P., and Remington, B. A., "An Evaluation of the Richtmyer-Meshkov Instability in Supernova Remnant Formation," *The Astrophysical Journal*, Vol. 511, No. 1, 1999, pp. 335–340.
doi:10.1086/306685

[12] Mueller, C. J., Driscoll, J. F., Reuss, D. L., Drake, M. C., and Rosalik, M. E., "Vorticity Generation and Attenuation as Vortices Convect Through a Premixed Flame," *Combustion and Flame*, Vol. 112, No. 3, 1998, pp. 342–358.
doi:10.1016/S0010-2180(97)00122-3

[13] Sinibaldi, J. O., Mueller, C. J., Tulkki, A. E., and Driscoll, J. F., "Suppression of Flame Wrinkling by Buoyancy: The Baroclinic Stabilization Mechanism," *AIAA Journal*, Vol. 36, No. 8, 1998, pp. 1432–1438.
doi:10.2514/2.534

D. Talley
Associate Editor